# Effect Of pH On The Physicochemical Properties Of MoVTeNbOx Catalysts For Oxidation Of Propane To Acrylic Acid

Syazwani M.N, Irmawati R, Taufiq-Yap Y.H, Zainuddin, N.

**Abstract**: $Mo_{1.0}V_{0.3}Te_{0.23}Nb_{0.12}$ mixed metal oxide catalysts were prepared via slurry method followed by microwave irradiation. The pH (1, 3, 5, and 7) of the synthesis solution was shown to affect physicochemical properties of the catalysts. XRD analysis revealed that the monophasic orthorhombic M1 phase $Te_2M_{20}O_{57}$ (M = Mo, V, and Nb) was only developed when pH was 1. This catalyst displayed BET surface area, 18.0 m$^2$/g the highest among other samples after post treatment and suggested the elimination of hexagonal M2 phase. The sample was also highly reducible with reduction temperature coincide very well with the temperature of catalytic reaction. Therefore, this catalyst was also active and selective for anaerobic propane oxidation to acrylic acid.

**Index Terms**: microwave-assisted, MoVTeNbOx mixed metal oxide, pH, post treatment, propane oxidation

————————————————◆————————————————

## 1 INTRODUCTION

LOWER alkanes (C1-C4) are a global affluent revenue from the natural gas and petroleum refinery off-gases. In the recent time, much effort has been attempted to convert these alkanes into more beneficial petrochemicals or feedstocks in the development of novel selective oxidation catalysts [1]. This great interest is due to their possible application as a feedstock of low cost raw materials especially for replacing corresponding olefins. Among selective oxidations of alkane, the conversion of propane to acrylic acid have gained focus of comprehensive research worldwide since the early of 1990s [1]. Nowadays, the major industrial acrylic acid production is via the catalytic partial oxidation of propylene [1]. This industrial process required acrylic acid production via a two-step process by converting propylene to acrolein and then followed by oxidation of acrolein to acrylic acid [1,2]. However, propane can be used alternatively as a feedstock by replacing its olefin through one-step oxidation process to directly produce acrylic acid [1]. The most promising catalyst to accomplish this one-step conversion is the multicomponent Mo-V-Te-Nb-O system which has been revealed as highly active and selective catalyst for the propane oxidation to acrylic acid [1, 3, 4, 5, 6]. The catalytically active center of the MoVTeNbOx system comprises of two crystalline phases which are orthorhombic M1 phase $Te_2M_{20}O_{57}$ (M = Mo, V, and Nb) and hexagonal M2 phase $Te_{0.33}MO_{3.33}$ (M = Mo, V and Nb) [7]. The orthorhombic M1 phase consists of an organization of octahedra and pentagonal bipyramidal [8]. MO6 octahedra (M = Mo, V) are assembled into layers in the ab-plane while hexagonal and heptagonal channels with the channels are partially filled with TeO units, meanwhile niobium fully occupies pentagonal bipyramidal sites.

The M2 phase is described as an orthorhombic structure possessing hexagonal channels only. The framework octahedra are partially occupied by V and Nb, whereas Te is accommodated in the channels [4]. The major dissimilarity exists among these two phases is that the M1 phase contains $V^{5+}$ centers, which are absent in M2 phase. In fact, this is one of the main reasons why the M1 phase is capable of activating propane [4, 8]. There have been several parameters considered in the synthesis of the complex multicomponent MoVTeNbOx catalyst. In particular, it has been reported that the formation of catalytic phase depends strongly on the synthesis pH [9, 10,11]. The pH of the synthesis solution may affect the crystallinity of catalyst and induced the formation of $(NH_4)_6TeMo_6O_{24}.nH_2O$, an Anderson-type heteropolyanions [9]. Besides, the variation in pH may also affect the of $MoO_3$ content, which is known to be inactive in propane oxidation [11]. In this work, the synthesis of multicomponent MoVTeNbOx will be done by utilizing microwave assisted synthesis method. The pH of the slurry will be varied as one of a critical factor controlling the phase composition and its effect on the physicochemical properties of the catalysts will be discussed.

## 2 EXPERIMENTAL SECTION

### 2.1 Catalyst Preparation

$Mo_{1.0}V_{0.3}Te_{0.23}Nb_{0.12}O_x$ catalysts were prepared by a slurry method followed by microwave irradiation according to the patented procedure (Malaysian patent pending file number 2011003855) [12]. The metal sources for Mo, V, Te and Nb were derived from ammonium heptamolybdate tetrahydrate, $(NH_4)_6Mo_7O_{24}.4H_2O$ (Merck), ammonium metavanadate, $NH_4VO_3$ (Merck), telluric acid, $Te(OH)_6$ (Sigma-Aldrich) and ammonium niobium oxalate, $(NH_4)_2Nb_2(C_2O_4)_5$ (Sigma-Aldrich), respectively. Firstly, ammonium heptamolybdate tetrahydrate were dissolved in a 15 ml of irradiated deionized $H_2O$. Then, the solution was irradiated for 3 min before ammonium metavanadate was added. The solution was then irradiated for another 3 min again. Telluric acid was later added and followed by the addition of irradiated ammonium niobium oxalate solution that were separately prepared using ammonium niobium oxalate dissolved in 5 ml of deionized $H_2O$ to the MoVTe suspension that was irradiated earlier. Finally, the resulting orange slurry formed were irradiated for 3 min.

————————————————————————

- *Syazwani Mohd Noor is currently pursuing a Master of Science in Catalysis in Universiti Putra Malaysia. E-mail: azwanisy@gmail.com*
- *Assoc. Prof. Dr. Irmawati Ramli; Department of Chemistry, Faculty of Science, Universiti Putra Malaysia. E-mail: irmawati@upm.edu.my*

The pH of precursor solution was taken using Thermo-line PHS-3BW digital pH meter and gave the value of 4.5 (±0.05). The pH of the solution was adjusted by using 1 M aqueous sulfuric acid for pH 1 and 3, and 1 M of an aqueous ammonium hydroxide for pH 5 and 7. It was then left for overnight and later dried using a rotary evaporator at 353 K. The precursors obtained were then heat treated for 1 h in air at 553 K and 2 h in $N_2$ at 873 K. The calcined samples were labelled as $MVTN_{xc}$, where $x$= 1, 3, 5, and 7 denoting the pH of the solution. Post-treatment was done by washing the solids using 30% $H_2O_2$ under vigorous stirring for 3 hours at the ratio of 1 g of catalyst to 10 ml of $H_2O_2$. The solid was separated from its liquid by centrifuging for 10 mins. The solid was collected and rinsed with deionized water for 5 times before drying for overnight at 353 K in an oven. These samples were then labelled as $MVTN_{xw}$, where $x$= 1, 3, 5, and 7 denoting the pH of the solution.

## 2.2 Catalyst Characterization

Powder XRD patterns were collected by using a Shimadzu Model XRD 6000 Diffractometer. Diffraction patterns were produced by employing $CuK_\alpha$ radiation with wavelength, $\lambda$= 1.542 Å which were continuously scanned at 2° $min^{-1}$ of scanning rate in the range of $2\theta = 2°$- 60°. The crystallite size was calculated using the Debye Scherrer equation. The $S_{BET}$ was done using Thermo Finnigan Sorptomatic apparatus. The sample being degassed overnight at 423 K and surface area was determined at analysis step where the degassed samples were subjected to $N_2$ adsorption at 77 K. The bulk composition of the sample was analyzed using ICP-AES model Perkin Elmer Emission Spectrometer Plasma 1000. The elemental composition of each sample was determined by digesting 0.025g of sample in aqueous 2% sulfuric acid ($H_2SO_4$) solution under heated condition. The resulting solution was diluted with deionized water to 250 ml and a range of standard solution of Mo, V, Te and Nb were prepared. The surface morphology of samples was investigated using Nova 200 NanoLab Field Emission Scanning Electron Microscope (FE-SEM) at an accelerating voltage of 5.0 kV. The aluminium stud with the carbon paint was initially prepared and tapped on the sample. Then, the stud was coated with gold. The $H_2$-TPR analysis was carried out using Thermo Finnigan TPDRO 1110 Instrument. The catalysts were perpetrated by heating the sample to 423 K under a $N_2$ flow at a heating rate of 10 K $min^{-1}$. After which, the $N_2$ gas flow was switched to 5% $H_2$/Ar and temperature programming from 323 K up to 1223 K at the heating rate of 10 K $min^{-1}$.

## 2.3 Anaerobic Propane Oxidation

Anaerobic propane oxidation was performed by Temperature Programmed Reaction (TPRn) analysis using Thermo Finnigan TPDRO 1110 Instrument. Before subjecting the catalyst to reaction gas, $N_2$ was flowed over the catalyst at 25 $min^{-1}$ for 30 min to remove any impurities from the catalyst surface. The flow was then switched to 5% $C_3H_8$/He (1 bar and 10 $cm^3$ $min^{-1}$) and temperature programming from 323 to 1223 K at the heating rate of 10 K $min^{-1}$. Mass spectrometer (Pfeiffer OmniStar) which is capable of monitoring multiple masses continuously with time was used to detect the output gas composition. The online mass spectrometer records propane (m/z=29), propylene (m/z= 41), $CO_2$ (m/z= m/z=44), acrolein (m/z=56), and acrylic acid (m/z=72).

# 3 RESULTS AND DISCUSSION

## 3.1 Catalyst Characterization

The XRD patterns of calcined catalysts ($MVTN_{1c}$, $MVTN_{3c}$, $MVTN_{5c}$ and $MVTN_{7c}$) are presented in Fig. 1. The presence of orthorhombic M1 phase $Te_2M_{20}O_{57}$ ($M$ = Mo, V, and Nb) can be seen from the peak patterns at $2\theta = 6.6°$, 7.9°, 9.0°, 22.1° and 45.0° (JCPDS: 58-790). While diffractions at $2\theta = 22.1°$, 28.3°, 36.2° and 50.0° suggests the presence of hexagonal M2 phase $Te_{0.33}MO_{3.33}$ (M = Mo, V and Nb) (JCPDS: 57-1099). There are also peaks found at $2\theta = 7.7°$, 8.9°, 22.1°, 24.2° and 31.3° which can be correlated to the existence of tetragonal phase, $(V_{0.07}Mo_{0.93})_5O_{14}$ (JCPDS: 31-1437).



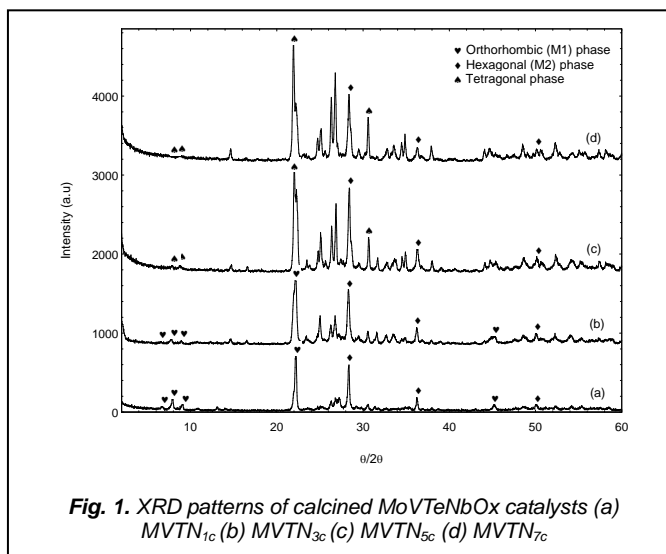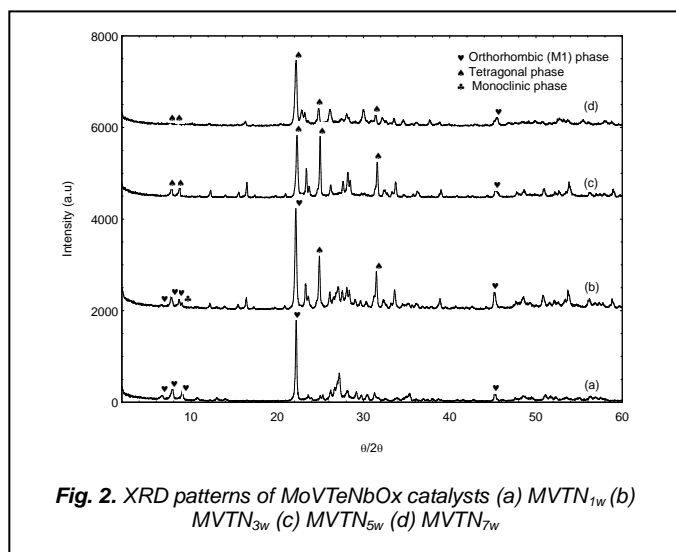**Fig. 1.** *XRD patterns of calcined MoVTeNbOx catalysts (a) $MVTN_{1c}$ (b) $MVTN_{3c}$ (c) $MVTN_{5c}$ (d) $MVTN_{7c}$*

It has been reported that the formation of these mixed phases was due to the presence of ammonium containing phases in the precursor [13] which later contributed to the formation of Anderson-type heteropoly-compounds (HPC) $(NH_4)_6TeMo_6O_{24}.7H_2O$, $(NH_4)_7TeMo_5O_{24}.8H_2O$ and $(NH_4)_8(V_{19}O_{41}$ (OH)$_9$ ($H_2O$)$_{11}$ [9,13]. These HPC compounds were crystallized to the respective phases when calcined in nitrogen. When the catalysts were post-treated with $H_2O_2$, some phase changes occur as can be seen in Fig. 2 ($MVTN_{1w}$, $MVTN_{3w}$, $MVTN_{5w}$ and $MVTN_{7w}$). The hexagonal M2 phase $Te_{0.33}MO_{3.33}$ (M = Mo, V and Nb) is no longer present as it was dissolved during the washing process. This happened through the dissolution of Te located on the hexagonal channel. $H_2O_2$ penetrates into this channel and hydroxylation reaction takes place [14]. The process can be represented as in (1).

$$M_a\text{-OH} + M_b\text{-OH} \longrightarrow M_a\text{-O-}M_b + H_2O$$

$$M_a\text{-O-}M_b + H_2O_2 \longrightarrow M_a\text{-OH} + M_b\text{-OH} + 1/2\ O_2$$

(1)

Where $M_a$ and $M_b$ corresponding to neighboring metal cations lining the heptagonal channel. The peaks observed at $2\theta = 6.7°$, 7.9°, 9.0°, 22.1°, 27.2° and 45.1° are all indexed to the orthorhombic M1 phase $Te_2M_{20}O_{57}$ ($M$ = Mo, V, and Nb) (Pba2) with unit cell parameters a = 2.11 nm, b = 2.66, c = 0.401 nm [8]. This is only found occur in $MVTN_{1w}$ which signify the monophasic nature of the catalyst as the consequence of low pH during the synthesis step. The rest of the post-treated catalysts may still contain other phases which are monoclinic

phase, $TeMo_5O_{16}$ phase (JCPDS: 31-0874), contributed by the introduction of the hydroxyl group into the compound and tetragonal phase, $(V_{0.07}Mo_{0.93})_5O_{14}$.



**Fig. 2.** *XRD patterns of MoVTeNbOx catalysts (a) MVTN$_{1w}$ (b) MVTN$_{3w}$ (c) MVTN$_{5w}$ (d) MVTN$_{7w}$*

BET surface areas of post-treated catalysts are shown in Table 1. Low surface areas (0.1 – 9.5 m$^2$/g) are observed in all catalysts except for MVTN$_{1w}$ which was prepared at pH 1 (18.0 m$^2$/g). It is clear that the pH of synthesis solution has strong effects on the physicochemical properties of the catalyst. The crystallite size was estimated by using the Debye Scherrer equation (2) using the full width at half maximum (FWHM) of the orthorhombic M1 phase peak at 2θ = 6.6°, 7.9° and 9.0°. These three peaks were chosen because it is the signature peaks for the orthorhombic M1 phase of the MoVTeNbOx catalyst [8]. The crystallite size value of 23.81 nm for MVTN$_{1w}$ corresponding very well with the high surface area of the catalyst.

$$t = \frac{0.9\lambda}{\beta_{hkl} \cos \Theta_{hkl}}$$                    (2)

Where t is the crystallite size, λ is 1.5438 Å, θ is the Bragg angle and β$_{hkl}$ is the full width at half maximum (FWHM) of the peak in radian. The results of the quantitative ICP analysis given in Table 1 indicate the bulk chemical compositions of post-treated catalysts as compared to their theoretical composition. The vanadium content in MVTN$_{1w}$ corresponding very well to the preparative composition of the MoVTeNbOx catalyst system. Lower concentration of vanadium that are found in other catalysts shows that the samples may contain mixed phases as coincide well with the FE-SEM images in Fig.3. This result signifies that a definite amount of vanadium is needed to accomplish a single M1 phase orthorhombic structure [15]. A noticeable loss of tellurium contents is observed in all samples in the bulk composition. In this way, a possible answer could be related to the presence of the reducing agent which is oxalate anions from the Nb metal source [16]. The melting point of Te metal is 723 K and the calcination at 873 K in nitrogen flow has caused the reduction of oxide of Te into Te metal [16]. This phenomenon was observed after calcination was completed when metallic Te was found deposited at the bottom of calcination tube. Meanwhile, the Nb content is also found lower in all samples.

However, the presence of Nb is found rather constant implying the stability of the element in the solid structure.

**Table 1.** *Elemental composition, BET surface area and crystallite size of MoVTeNbOx catalysts of MVTN$_{1w}$, MVTN$_{3w}$, MVTN$_{5w}$ and MVTN$_{7w}$*

| Sample | Crystallite size (nm) | S$_{BET}$ (m$^2$/g) | Bulk composition[1] (Mo: V: Te: Nb) |
|--------|------------|-----------|--------------------|
| MVTN$_{1w}$ | 23.81 | 18.0 | 1.0: 0.27: 0.09: 0.06 |
| MVTN$_{3w}$ | 32.25 | 9.5 | 1.0: 0.17: 0.09: 0.03 |
| MVTN$_{5w}$ | NA$^2$ | 3.0 | 1.0: 0.18: 0.12: 0.07 |
| MVTN$_{7w}$ | NA$^2$ | 0.1 | 1.0: 0.20: 0.12: 0.07 |

*Preparative composition of Mo: V: Te: Nb = 1.0: 0.3: 0.23: 0.12*
[1]*Determined by ICP-AES*

FESEM images (Fig. 3) of the catalysts show that the morphology of the orthorhombic M1 phase, existing as monophase in MVTN$_{1w}$ is platelet-like with uniform size distribution [17]. A mixture of the rod-like and platelet-like morphology is observed in the other samples which is consistent with the mixed phases nature of the catalysts.



Fig. 3. FE-SEM image of washed MoVTeNbOx catalysts (a) MVTN$_{1w}$ (b) MVTN$_{3w}$ (c) MVTN$_{5w}$ (d) MVTN$_{7w}$
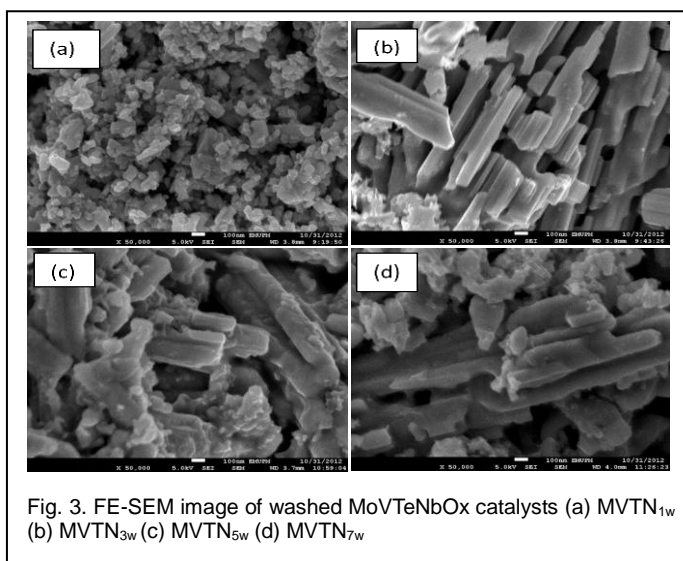
The H$_2$-TPR profiles of post-treated catalysts are shown in Fig. 4. The analysis allows the hydrogen to be in contact with the oxygen species from the surface of the catalyst. The reaction between hydrogen and oxygen species occurs and forms water as a product. This will leave an oxygen vacancy on the catalysts. The interaction between gas phase hydrogen with oxygen species can be represented in (3).

(3)          $H_{2(g)} + O_{(s)} \longrightarrow H_2O_{(g)} + \square$
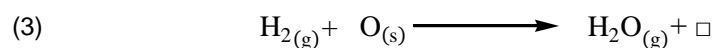
Where (g), (s) represent gaseous or surface species and □ is oxygen vacancy. The interaction of the hydrogen with the surface oxygen can be described according to the Eley-Rideal mechanism. At high temperature, hydrogen impinges on the surface oxygen species, thereby forming a bond with the oxygen. Surface reaction between both species occurs and formed water as the product. The product water was later

desorbed to the gas phase and leaving behind an oxygen vacancy on the catalyst surface. The amount of oxygen removed can be obtained by calculating the area under the peak and the reduction activation energy of the catalyst can be calculated using the modified version of the Redhead equation as shown in the (4).

$$\frac{E_r}{RT_m{}^2} = \left(\frac{A_r}{\beta}\right)[H_2]_m \exp\left(\frac{-E_r}{RT_m}\right) \qquad (4)$$

Where $T_m$ is the peak maximum temperature (K) in the rate of production of $H_2$, $E_r$ is the reduction activation energy (kcal mol$^{-1}$), $A_r$ is the reduction pre-exponential term (cm$^3$mol$^{-1}$s$^{-1}$) which is given a standard collision number of $10^{13}$ cm$^3$ mol$^{-1}$s$^{-}$, $\beta$ is the heating rate (Ks$^{-1}$) and $[H_2]_m$ is the gas phase concentration of hydrogen (mole cm$^{-3}$) at the peak maximum.

For sample MVTN$_{1w}$, three reduction peak occurred at maximum temperature of 820 K, 868 K and 1042 K. Meanwhile, MVTN$_{3w}$ shows a double peak with its maximum centered at temperature 824 K and 912 K, and at 842 K and 1045 K for MVTN$_{7w}$. Meanwhile, MVTN$_{5w}$ shows one peak maximum at 994 K.
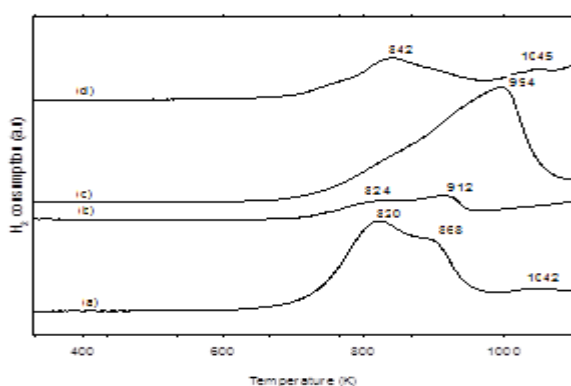


**Fig. 4.** $H_2$-TPR profiles of washed MoVTeNbOx catalysts (a) MVTN$_{1w}$ (b) MVTN$_{3w}$ (c) MVTN$_{5w}$ (d) MVTN$_{7w}$

Although there is no clear trend in the reduction profiles, but an important point to be noted is the peak maxima for MVTN$_{1w}$ is lower with big size peak indicating of the highly reducibility of this catalyst compared to others. The total amount of removable oxygen in this catalyst is the highest as can be seen in Table 2. The reduction activation energy, $E_r$ is > 100 kJ mol$^{-1}$ signify that the origin of the oxygen species were from the surface and lattice of the catalyst.

| Sample | T$_{max}$ (K) | Reduction activation energy, Er (kJ mol$^{-1}$) | Total O$_2$ removed (atom g$^{-1}$) ×10$^{21}$ |
|---|---|---|---|
| MVTN$_{1w}$ | 820 | 137.0 | 6.08 |
| | 868 | 145.0 | 2.91 |
| | 1042 | 174.1 | 0.33 |
| | | | Total: 9.32 |
| MVTN$_{3w}$ | 824 | 137.7 | 0.71 |
| | 912 | 152.4 | 1.12 |
| | | | Total: 1.83 |
| MVTN$_{5w}$ | 994 | 166.1 | 13.16 |
| | | | Total: 13.16 |
| MVTN$_{7w}$ | 842 | 140.7 | 1.92 |
| | 1045 | 174.6 | 0.48 |
| | | | Total: 2.40 |

**Table 2.** The reduction activation energy, $E_r$ and total O$_2$ removed determined from $H_2$-TPR for MVTN$_{1w}$, MVTN$_{3w}$, MVTN$_{5w}$, and MVTN$_{7w}$.

The oxygen species are originated from the metal oxides as has been reported that MoO$_n$ reduced at 948 K and 995 K for a stepwise reduction of Mo$^{6+}$ → Mo$^{4+}$ and Mo$^{4+}$ → Mo$^0$. Meanwhile VO$_n$ reduced at temperature of 913 K and 943 K from V$^{5+}$→ V$^{4+}$ [19]. The conditions of a multiple reduction peaks suggesting the kinetically different of oxygen species present in the catalyst.

## 3.2 Anaerobic propane oxidation
The catalytic response obtained in the form of a mass spectrogram of the respective m/z that was followed and analyzed quantitatively. The analysis was done on MVTN$_{1w}$ because this is the only catalyst which possessed orthorhombic M1 phase. Fig. 5 shows the TPRn profile of MVTN$_{1w}$.
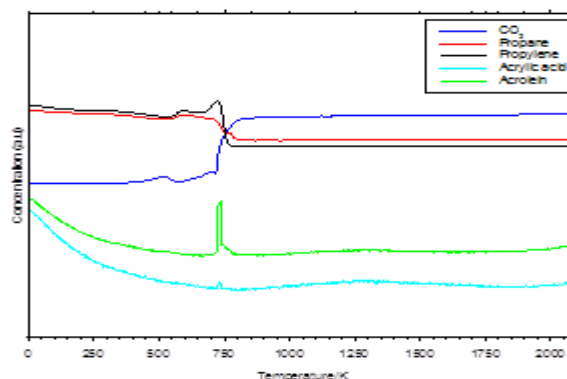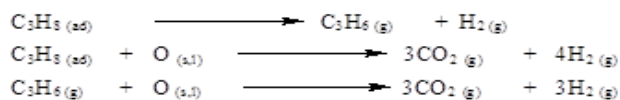


**Fig. 5.** TPRn profile of anaerobic propane oxidation for MVTN$_{1w}$

The reaction was found to begin immediately after propane was flowed over the catalyst as dictated by the decrease of propane concentration at the beginning of the temperature programming until 600 K. This is due to the physical adsorption of a propane molecule on the surface of the catalyst. Afterward, the propane curves climbing until it reaches a maximum at around 650 K. Thus, when it was desorbed as shown as a peak maximum at 650 K it was still in its molecular property as described in the (5).

$$C_3H_{8\,(g)} \longrightarrow C_3H_{8\,(ad)}$$
$$C_3H_{8\,(ad)} \longrightarrow C_3H_{8\,(g)} \qquad (5)$$
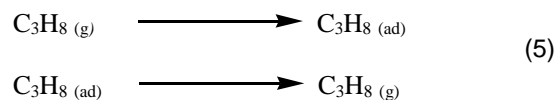
Where (g) and (ad) denotes gaseous and adsorbed species. However, close inspection of the profile indicates that a CO$_2$ signal with a peak at 600 K is observed. Hence, whereas the majority of propane evolved as propane molecule (physical adsorption) but some of the molecules was strongly attached to the catalyst surface forming bonds with the surface oxygen. Thereafter, bond breakage occurs forming CO$_2$ as the product. Besides, a dehydrogenation reaction is also happening as evidenced by the evolution of propylene in the same temperature range. Scheme 1 described the proposed chemical equation for the process involved. The oxygen species that were used for propane bonding, C-C bond breakage and eventually released as CO$_2$ as shown in the Scheme 1 are not the selective ones, although it is active for the reaction. This is because there is no desired product which is acrylic acid evolved during the reaction. The temperature for oxygen being taken up by propane coincide very well with the hydrogen reduction temperature indicating that the same

43

oxygen species were involved in this step of the reaction.

$$C_3H_{8\,(ad)} \longrightarrow C_3H_{6\,(g)} + H_{2\,(g)}$$
$$C_3H_{8\,(ad)} + O_{(s,l)} \longrightarrow 3CO_{2\,(g)} + 4H_{2\,(g)}$$
$$C_3H_{6\,(g)} + O_{(s,l)} \longrightarrow 3CO_{2\,(g)} + 3H_{2\,(g)}$$

*Scheme 1. Proposed reaction of propane dehydrogenation and propane oxidation. Where (g) = gaseous species, (ad) = adsorbed species, (s,l) = surface or lattice oxygen*

Afterwards, the propane signal shows a decrease continuously until the end of the temperature programming. The propane signal is mirrored by the $CO_2$ signal which signify the continuous production of $CO_2$ as propane was flowed over the catalyst. It should follow the same reaction process as shown in Scheme 1. Therefore, the oxygen used for insertion into $CO_2$ is not the selective ones. Interestingly, at this high temperature of the reaction, a curve belongs to acrylic acid is appeared. A rather broad peak is seen to be evolved in this temperature range with a peak maximum at 1250 K. This temperature dependence of acrylic acid production is similar with the temperature dependence of acrolein production. The reaction is proposed to occur in a step-wise manner as proposed in the Scheme 2. Propane, ($C_3H_8$) as a starting reaction was dehydrogenated to form propylene, ($C_3H_6$). It was later converted to acrolein, $CH_2=CHCHO$ by an oxygen insertion. Finally, another insertion of oxygen on acrolein gives acrylic acid as desired products. What is noticed, $CO_2$ is continuously produced in all steps, due to the C-C bond breakage occurs on the catalyst surface.

$$C_3H_8 \longrightarrow C_3H_6 \longrightarrow CH_2=CHCHO \longrightarrow CH_2=CHCOOH$$
$$CO_2$$
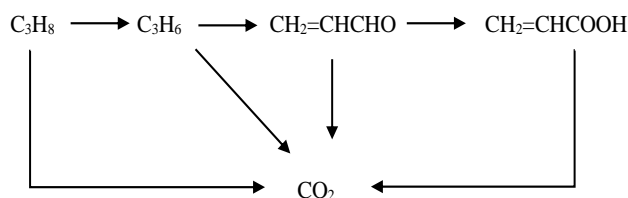
*Scheme 2. Proposed reaction scheme of anaerobic oxidation of propane of MoVTeNbOx catalysts synthesized in this work*

## 4 CONCLUSION

MoVTeNbOx catalysts prepared by varying their synthesis pH present a catalyst with various physicochemical properties. It has been found that pH 1 is the best pH for obtaining monophasic orthorhombic M1 phase $Te_2M_{20}O_{57}$ ($M$ = Mo, V or Nb). Other pH (3, 5 and 7) gave a mixed phases oxides that were inactive for propane activation. The catalyst also has superior properties compared to others in term of its high BET surface area and highly reducible property which is needed for an oxidation reaction. The catalyst also gave a good catalytic performance when tested in an anaerobic propane oxidation reaction due to its ability to remove high amounts of oxygen.

## REFERENCES

[1] Lin, M. M. (2001). Selective oxidation of propane to acrylic acid with molecular. Applied Catalysis A: General, 207: 1–16.

[2] Voge, H. H., and Adams, C. R. (1967). Catalytic oxidation of olefins. Advances in Catalysis, 17:151.

[3] Yu, Z., Zheng, W., Xu, W., Zhang, Y., Fu, H., and Zhang, P. (2009). Effect of preparation conditions on selective oxidation of propane to acrylic acid. Transactions of Nonferrous Metals Society of China, 19:476-479.

[4] Beato, P., Blume, A., Girgsdies, F., Jentoft, R.E., Schlögl, R., Timpe, O., Trunschke, A., Weinberg, G., Basher, Q., Hamid, F.A., Hamid, S.B.A., Omar, E., and Mohd Salim, L. (2006). Analysis of structural transformations during the synthesis of a MoVTeNb mixed oxide catalyst. Applied Catalysis A: General, 307(1):137-147.

[5] Ueda, W., Vitry, D., Katou, T., Watanabe, N., and Endo, Y. (2006). Key aspects of crystalline Mo-V-O-based catalysts active in the selective oxidation of propane. Research on Chemical Intermediates, 32(3-4): 217-233.

[6] Ushikubo, T., Nakamura, H., Koyasu, Y., and Wajiki, S. (1995). Method for producing an unsaturated carboxylic acid. Patent 5 380 933.

[7] Ushikubo, T., Oshima, K., Kayou, A., and Hatano, M. (1997). Ammoxidation of propane over Mo-V-Nb-Te mixed oxide catalysts. Studies in Surface Science and Catalysis, 112:473-480.

[8] Grasselli, R.K., Buttrey, D.J., DeSanto Jr, P., Burrington, J.D., Lugmair, C.G., Volpe Jr, A. F., and Weingand, T. (2004). Active centers in Mo–V–Nb–Te–Ox (amm)oxidation catalysts. Catalysis Today, 91–92: 251-258.

[9] Oliver, J.M., López Nieto, J.M., Botella, P., and Mifsud, A. (2004). The effect of pH on structural and catalytic properties of MoVTeNbO catalysts. Applied Catalysis A: General, 257(1): 67-76.

[10] Guan, J., Wang, H., Yang, Y., Liu, B., Yu, X., Ma, Y., and Kan, Q. (2009). Effect of pH on the catalytic properties of Mo–V–Te–P–O catalysts for selective oxidation of isobutane. Catalysis Letters, 131(3-4):512-516.

[11] Yu, Z., Zheng, W., Xu, W., Zhang, P., Fu, H., and Zhang, Y. (2011). Crystalline structure of mixed metal oxide catalysts for propane selective oxidation to acrylic acid. Transactions of Nonferrous Metals Society of China, 21(2):405-411.

[12] Irmawati, R., Muda, A. A., Ismail, A.Z., and Ahangar, H.A. (2011). Patent Pending no PI2011003855.

[13] Sanfiz, A.C., Hansen, T.W., Girgsdies, F., Timpe, O., Rodel, E., Ressler, T., Trunschke, A., and R. Schlogl, R. (2008). Preparation of phase-pure M1 MoVTeNb oxide catalysts by hydrothermal synthesis—Influence of reaction

44

parameters on structure and morphology. Topics in Catalysis, 50:19–32.

[14] Deniau, B., Bergeret, G., Jouguet, B., Dubois, J.L., and Millet, J.M.M. (2008). Preparation of single M1 phase MoVTe(Sb)NbO catalyst: Study of the effect of M2 phase dissolution on the structure and catalytic properties. Topics in Catalysis, 50(1-4):33-42.

[15] Vitry, D., Morikawa, Y., Dubois, J.L., and Ueda, W. (2003). Mo-V-Te-(Nb)-O mixed metal oxides prepared by hydrothermal synthesis for catalytic selective oxidations of propane and propene to acrylic acid. Applied Catalysis A: General, 251: 411-424.

[16] Ivars, F., Solsona, B., Hernández, S. and López Nieto, J.M. (2010). Influence of gel composition in the synthesis of MoVTeNb catalysts over their catalytic performance in partial propane and propylene oxidation. Catalysis Today, 149:260-266.

[17] Lin, M. M. (2003). Complex metal oxide catalysts for selective oxidation of propane and derivatives: II. The relationship among catalyst preparation, structure and catalytic properties. Applied Catalysis A: General, 250:287-303.

[18] Jiang, H. C., Lu, W. M., and Wan, H. L. (2004). The effect of $MoV_{0.3}Te_{0.23}P_xO_n$ catalysts with different phosphorus content for selective oxidation of propane to acrolein. Journal of Molecular Catalysis A-Chemical, 208: 213-217.